ELSEVIER

Journal of Structural Geology 29 (2007) 1339–1352

JOURNAL OF STRUCTURAL GEOLOGY

www.elsevier.com/locate/jsg

# Characterization of the Monument Hill fault system and implications for the active tectonics of the Red Rock Valley, Southwestern Montana

Christine A. Regalla*, David J. Anastasio, Frank J. Pazzaglia

*Lehigh University, Department of Earth and Environmental Sciences, Bethlehem, PA 18015-3126, USA*

Received 1 September 2006; received in revised form 3 April 2007; accepted 5 April 2007
Available online 7 May 2007

**Abstract**

New geologic mapping, morphologic fault scarp modeling, and geomorphic metrics in the Red Rock Valley, southwestern Montana, help characterize the Quaternary history of the virtually unstudied Monument Hill fault and tectonics of the youthful and seismically active Red Rock graben. Two generations of Pleistocene surface ruptures are preserved along the Monument Hill fault. Similarity in rupture ages along multiple strands, determined from offset alluvial surfaces and morphologic modeling, suggest earthquake clusters at 22–32 ka and possibly >160 ka. Quaternary activity along the Monument Hill fault is also reflected in elongate drainage basins and channel profiles with anomalously steep reaches coincident with mapped faults. An anticlinal accommodation zone at Kidd accommodates a change in fault polarity between the en echelon Monument Hill and Red Rock faults and a northward decrease in extension within the Red Rock graben. The unique rupture histories of the Monument Hill and Red Rock faults, however, suggest the systems are not seismogenically linked and that the accommodation zone serves as a rupture barrier. The geometry, interconnectivity, and kinematics of faults in the Red Rock Valley may represent a snapshot of the early stages of extension applicable to the evolution of other Northern Basin and Range grabens.


*Keywords:* Active tectonics; Basin and Range; Montana; Tectonic geomorphology

## 1. Introduction

Crustal extension, like that occurring within the northern Basin and Range, evolves through the interaction, linkage, and growth of smaller, individual faults (Dawers and Anders, 1995; Morley, 1999; McLeod et al., 2000). Fault growth, linkage and the potential to influence rupture patterns on adjacent faults have direct implications for the geometries of evolving extensional basins and for seismic hazard analyses. The recognition of earthquake clustering on several faults in the Basin and Range (e.g. Wallace, 1987; Olig et al., 1994, 1995; Hemphill-Haley et al., 1994; Knuepfer, 1994) calls for more detailed analyses of rupture histories, as long term recurrence intervals may be at a discordance with short-term rupture histories (e.g. Swan, 1988; Marco et al., 1996; Anderson et al., 2003) and with the modern seismic record (e.g. Stickney and Lageson, 2002). The northern Basin and Range province of southwestern Montana is a natural laboratory where the evolution of nascent extensional systems (e.g. Sears and Fritz, 1998; Harkins et al., 2005) and poorly described Quaternary faults (Anderson et al., 2003) can be studied. This paper utilizes new geologic mapping, a recently developed Quaternary stratigraphy for the Red Rock Valley (Harkins et al., 2005), morphologic dating of fault scarps, and analysis of geomorphic metrics to characterize the Quaternary activity of the virtually unstudied Monument Hill fault. Results are applicable to seismic hazard analyses and the interconnection, growth, and seismogenic linking between faults in the Red Rock Valley.

The Monument Hill fault is located within the Red Rock graben, a youthful, active extensional system on the eastern flank of the Northern Basin and Range Province (Fig. 1). The youth of the Red Rock graben is supported by the following

* Corresponding author. Present address: Pennsylvania State University, Department of Geosciences, 542 Deike Building, University Park, PA 16802, USA.

*E-mail addresses:* cregalla@geosc.psu.edu (C.A. Regalla), dja2@lehigh.edu (D.J. Anastasio), fjp3@lehigh.edu (F.J. Pazzaglia).

0191-8141/$ - see front matter 
doi:10.1016/j.jsg.2007.04.006

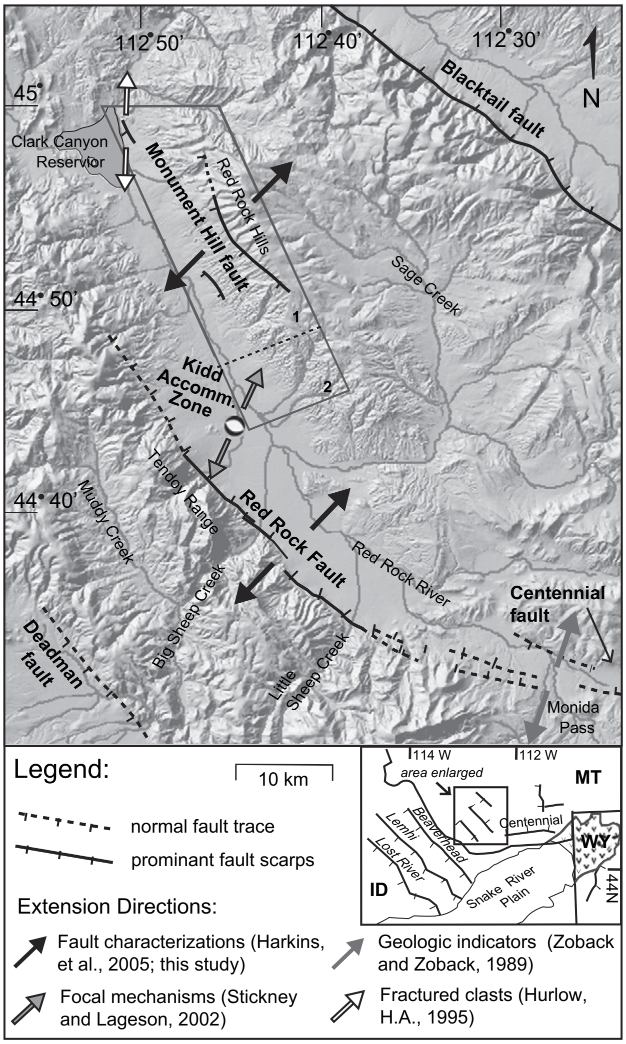


Fig. 1. Thirty-meter digital elevation model (DEM) of the Red Rock Valley and surrounding ranges showing the location of the Monument Hill fault system and regional faults, the focal mechanism for the 1999 Red Rock Valley earthquake, and regional extension directions. Inset map shows regional tectonic setting. Box 1 outlines area shown in Fig. 2; box 2 outlines area shown in Fig. 5. Figure adapted from Harkins et al. (2005).

observations: (1) faults in the Red Rock graben have limited strike-length and throw; (2) numerous hanging wall bedrock remnants are preserved in the valley; (3) the Red Rock Valley has only a thin veneer of Quaternary fill; (4) the range front topography of the Red Rock Hills is subdued, and the relief of the Tendoy Range is interpreted to be partially inherited from pre-extensional topography along the Sevier thrust front (Harkins et al., 2005). These observations, combined with historic seismic activity in the Red Rock Valley, collectively argue for an active Basin and Range extensional system in its early stages of development and imply that the graben may contain youthful faults. This study presents a combination of footwall, scarp, and hanging wall analyses that help characterize the Quaternary rupture history of the Monument Hill fault and, when integrated with existing data from the Red Rock Valley, help elucidate the geometry and tectonics of the Red Rock graben. The structure, interconnectivity, and kinematics of faults in the Red Rock Valley may represent a snapshot of the early stages of extension in the evolution of other Basin and Range grabens north of the Snake River Plain.

## 2. Seismic linkage, clustering, and accommodation zones

Strain transfer between faults within extensional systems like the Red Rock graben can lead to seismogenic linking (Stein, 1999; King et al., 1994; Di Bucci et al., 2006) and the triggering of earthquakes on adjacent faults due to post-seismic reloading and relaxation (Kenner and Simons, 2005; Chery et al., 2001a,b). The results are temporally clustered earthquakes (Lynch et al., 2003) a phenomena observed along many faults in the western United States that may be characteristic of regions with low effective viscosities in the non-seismogenic lithosphere, low strain accumulation rates, and large stress-drop earthquakes, such as the Basin and Range (Kenner and Simons, 2005). Clustering of large magnitude events implies non-steady long-term slip rates and variable recurrence intervals and must be taken into account to accurately assess seismic hazard and risk. Parameters important for hazard analyses, including measurements of rupture length and offset for the calculation of maximum magnitudes (Wells and Coppersmith, 1994), and rupture ages for the calculation of rupture recurrence intervals, have not previously been determined for the Monument Hill fault.

Field and analogue models show that extensional systems like the Red Rock graben are often characterized by fault segments or strands that change slip polarity across accommodation zones (Gibbs, 1984; Morley et al., 1990; Gawthorpe and Hurst, 1993; Faulds and Varga, 1998; Acocella et al., 2005; Hus et al., 2005). Accommodation zones transfer strain between overlapping half grabens or between fault segments and produce anticlinal and synclinal structures in the zone of overlap (Faulds and Varga, 1998; Morley et al., 1990; Gawthorpe and Hurst, 1993). Faults within accommodation zones evolve from underlapping faults, to overlapping faults and to eventual mechanical linkage (Acocella et al., 2000; Jackson et al, 2002; Peacock, 2002). Red Rock graben faults have rupture geometries that are typical of accommodation zones. At present, they are structurally immature where the moment magnitude release during an earthquake is limited by short strike lengths. Larger-magnitude earthquakes might be expected as the fault systems mature and link to longer, through-going structures. Because the geometry and evolution of accommodation zones are scale-independent and characterize both incipient and well-developed extensional basins (Acocella et al., 2000), observations made in the Red Rock graben are applicable to the larger grabens west of the Red Rock valley in the northern Basin and Range Province.

## 3. Tectonic setting and previous studies

The Northern Basin and Range Province in Idaho and Montana is characterized by northwest-trending, range-bounding normal faults that partition the landscape into a series of sediment-filled basins and fault block ranges. The Red

Rock Valley is a northwest-trending graben, bound on the southwest by the Red Rock fault, the range-bounding normal fault of the Tendoy Range, and on the northeast by the Monument Hill fault, located in the Red Rock Hills (Fig. 1). Extensional structures in the Red Rock Valley are superimposed on the McKenzie and Tendoy thrust sheets of the Montana recess in an area where Sevier structures are buttressed against the Laramide Blacktail-Snowcrest uplift (Skipp et al., 1989; McDowell, 1997; Janecke et al., 2002). Bedrock units in the Red Rock Valley include Mesozoic and Paleozoic carbonates and siliciclastics of the Tendoy and McKenzie thrust sheets, Mesozoic conglomerates of the Beaverhead Group, two generations of recycled, Tertiary, paleovalley-fill conglomerates, and Tertiary volcanic rocks (Haley and Perry, 1991; Schmitt et al., 1995; Kuenzi and Fields, 1971; Fields et al., 1985; Sears et al., 1995).

The Red Rock valley lies within the Centennial Tectonic Belt, a branch of the Intermontaine seismic belt that extends westward from Yellowstone National Park and encompasses parts of northwestern Wyoming, eastern Idaho, and southwestern Montana (Qamar and Stickney, 1983). This belt is host to two of the largest recorded intercontinental earthquakes in the United States, the 1983 Borah Peak earthquake (M 7.3) and the 1959 Hebgen Lake earthquake (M 7.5). Numerous smaller earthquakes are also recorded in the region daily. Recent local seismicity includes the 1999 Red Rock Valley earthquake (M 5.3) and the 2006 Dillon earthquake (M 5.6). The parabolic distribution of modern seismicity about the Snake River Plain has been attributed to the passage of the Yellowstone hotspot (Anders et al., 1989; Pierce and Morgan, 1992; Fritz and Sears, 1993; Bartholomew et al., 2002); however, the precise relation between Basin and Range extension and Yellowstone remains unresolved.

Despite the record of historic seismicity in the Red Rock valley, the Monument Hill fault is virtually unstudied and sparsely noted in the literature. Prior studies focused on the rupture history and segmentation of the Red Rock fault (Johnson, 1981; Haller, 1988; Greenwell, 1997; Harkins et al., 2005) but provide little information on recurrence intervals or geometry of the Monument Hill fault. The Monument Hill fault is described as the northernmost and most prominent section of the discontinuous, Red Rock Hills fault, with at least one large-magnitude earthquake in the Quaternary (Haller, 1993) and an estimated slip rate of <0.2 mm/year (Stickney, 2000). Previous mapping of the Monument Hill fault includes a 1:125,000 scale map showing offset undifferentiated Quaternary and Tertiary gravels (Scholten et al., 1955), and a 1:100,000 scale map (Lonn et al., 2000) showing offset late Pleistocene surfaces. A most recent rupture age of <130 ka for the Monument Hill fault is inferred based on morphology of a single scarp profile and the inferred age of faulted deposit (Ostenaa and Wood, 1990).

The Red Rock valley is interpreted as an asymmetric graben with a conjugate, normal fault geometry (Stickney and Lageson, 2002) bound on the northeast by the west-dipping Monument Hill fault and on the southwest by the east-dipping Red Rock fault (Fig. 1). This interpretation is consistent with fault-plane solutions for the 1999 Red Rock Valley earthquake, which place the hypocenter along a south-southwest-dipping fault in a complex structural cross-over zone between the Monument Hill and Red Rock faults (Stickney and Lageson, 2002). This interpretation is also consistent with a gravity gradient mapped within this cross-over zone that separates two structural sub-basins in the Red Rock Valley (Johnson, 1981).

## 4. Geologic mapping

### *4.1. Bedrock geology*

Bedrock and surficial mapping along the Red Rock Hills was completed at a scale of 1:24,000 with the aid of 1:30,000 scale aerial photos (Fig. 2). The footwall of the Monument Hill fault is comprised of conglomerate and volcanic rocks of the Cretaceous Beaverhead Group, Tertiary Renova Formation, and Tertiary Sixmile Creek Formation. The Beaverhead Group underlies the high standing topography of the Red Rock Hills and outcrops continuously in the footwall of the Monument Hill fault and discontinuously within the hanging wall (Newton et al., 2005; Regalla et al., 2006). The Beaverhead Group in the hanging wall of the Monument Hill fault is divided into three informal members: a lower, well-indurated, limestone gravel conglomerate; a thin, middle, dacitic volcanic unit; and a thick, upper, poorly indurated, quartzite conglomerate containing a well-indurated quartzite and limestone conglomerate lens (Haley and Perry, 1991; Schmitt et al., 1995; Regalla et al., 2006). The Paleozoic units of the McKenzie thrust sheet underlie the Red Rock Valley and occur in the hanging wall of the Monument Hill fault, but exposure is limited to a single outcrop south of Maurer Creek (Regalla et al., 2006).

### *4.2. Surficial geology*

Four alluvial deposits and their associated geomorphic surfaces have been defined along the Red Rock Hills, a refinement on the two deposits previously defined for this area (Lonn et al., 2000). Stratigraphy was developed on the basis of inset and burial relationships, surface morphology, and soil calcic horizon development. Soil pits were dug in the three oldest fan units and soil profiles were described to a depth of ~1 m. Soil carbonate development was characterized in these pits and from natural exposures using the stages of Gile et al. (1966). Datable organic material was not found in the Quaternary deposits on the eastern side of the Red Rock Valley so calcic horizon development, calibrated locally and regionally, was used for relative age (Gile et al., 1966; Birkeland, 1999). These soils were correlated to dated deposits on the opposite side of the valley (Harkins et al., 2005). Surface morphologic criteria—including the degree of bar and swale modification, the amount of incision by modern channels, and the relative type and abundance of vegetation—were used to characterize each geomorphic surface for correlation and mapping.

The oldest unit, Qaf1, underlies the highest elevation surfaces, approximately 10–12 m above the modern channel, and is inset by three younger alluvial units. The Qaf1 alluvial

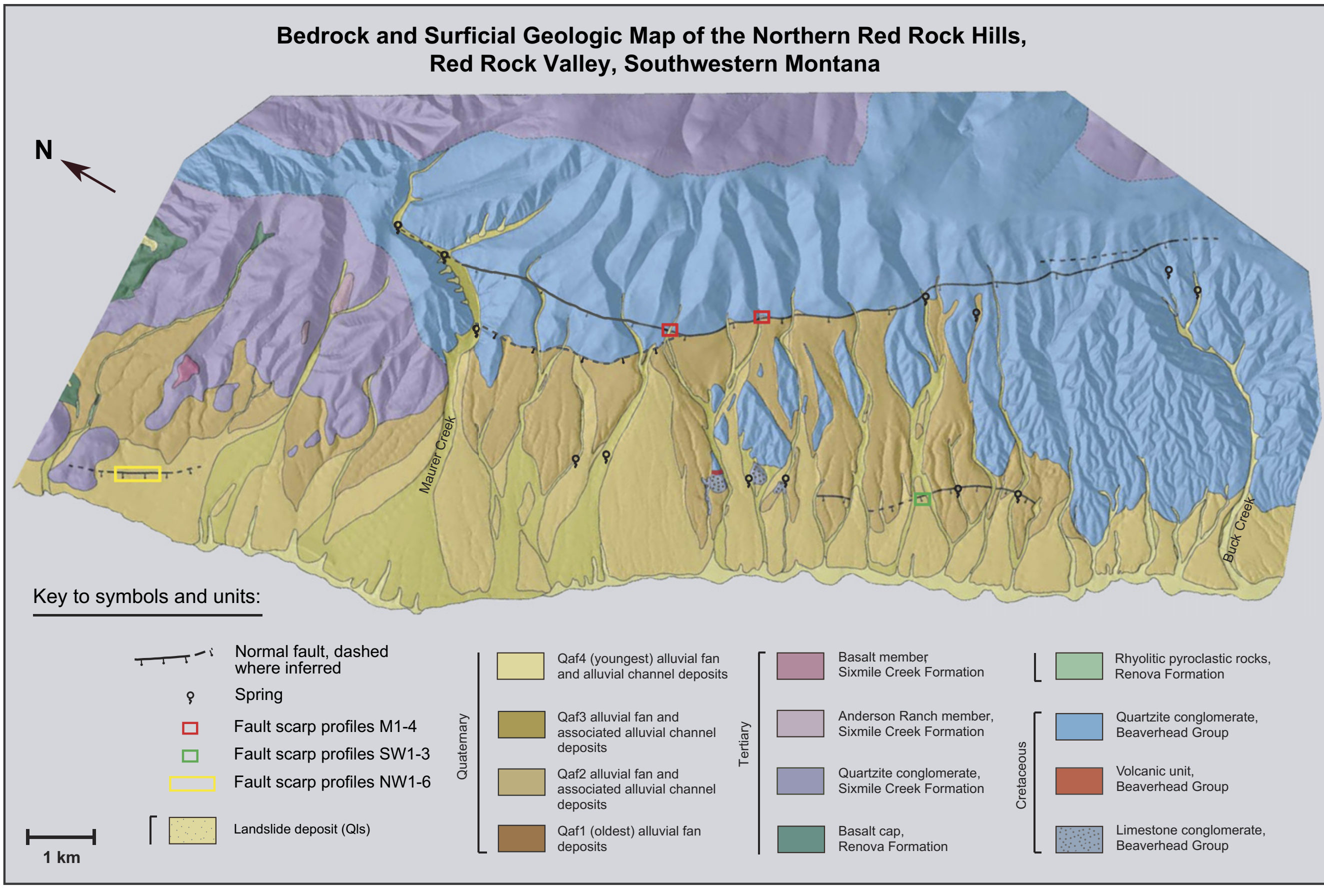


Fig. 2. Surficial and bedrock geology of the Red Rock Hills adjacent to the Monument Hill fault, Red Rock Valley, Southwestern Montana. See Fig. 1 for location.

surface is characterized by a lack of bar and swale morphology, a cover vegetation dominated by grass over sagebrush, a ~30 cm upper loess layer, highly weathered cobbles, and stage III to III+ calcic horizon development (Table 1). Qaf1 deposits are present at lower elevations along the southern half of the Monument Hill fault, projecting to an average elevation of ~1800 m (5900 ft) near Buck Creek and ~1890 m (6200 ft) near Maurer Creek (Fig. 2).

The second-oldest unit, Qaf2, lies 2–5 m above the modern channel and is inset into Qaf1 deposits. The surface is characterized by subdued bar and swale morphology, dominant grass with little sagebrush, and stage II+ to III calcic horizon development (Table 1). Qaf2 fans are restricted to elevations below ~1890 m (6200 ft) along the southern portion of the fault but extend up to elevations of 2133 m (7000 ft) near Maurer Creek (Fig. 2).

The third oldest unit, Qaf3, lies 1–2 m above the modern channel and is both inset into and buries Qaf2 deposits, depending on location along fault strike. Near Buck Creek, Qaf3 surfaces are inset as wide channels into Qaf2 and Qaf1

Table 1
Soil calcic horizon classification, descriptions of surface morphology, and ages of alluvial surfaces in the Red Rock valley

| Alluvial unit | Stage of soil carbonate development | Surface morphology | Radiocarbon age[a] | Age range |
|---|---|---|---|---|
| $Qaf_4$ | I to II | Unmodified bar and swale<br>Dominance of grass<br>Deeply incised (10–12 m) | 4560 ± 60 years | 5–3 ka Middle Holocene |
| $Qaf_3$ | II+ to III | Subdued bar and swale<br>Dominant grass, little sagebrush<br>Moderately incised (2–5 m) | 10480 ± 60 years | ~20–10 ka Latest Pleistocene |
| $Qaf_2$ | III + to III | Slightly modified bar and swale<br>Abundant grass, sagebrush<br>Minimal incision (1–2 m) | >50000 | ~130–160 ka Late Pleistocene |
| $Qaf_1$ | III to III+ | Lack of bar and swale<br>Dominance of grass<br>Inset into older fans | – | >160 ka Middle(?) Pleistocene |

[a] Ages determined by correlating fans along the Monument Hill fault to dated fans along the Red Rock fault (Harkins et al., 2005).

surfaces, while near Maurer Creek, Qaf3 surfaces bury older units and form large alluvial fans (Fig. 2). A Qaf3 surface is characterized by slightly modified bar and swale morphology, abundant grass and sagebrush, and stage I+ to II calcic horizon development (Table 1).

The youngest unit, Qaf4, is inset into the toe of Qaf3 and Qaf2 deposits in the valley below the Monument Hill fault (Fig. 2). The Qaf4 surface is the modern depositional surface and is characterized by unmodified bar and swale morphology, sparse sagebrush, and little to no accumulation of soil carbonate (Table 1).

Fan unit ages were estimated by correlating calcic horizon development and surface morphology to those of radiometrically dated fans on the southwest side of the Red Rock Valley. Charcoal samples from the two youngest fans along the southwestern flank of the valley yielded radiocarbon ages of $4560 \pm 60$ and $10480 \pm 60$ years (Harkins et al., 2005). These ages are used as minima and correspond to the Qaf4 and Qaf3 deposits along the Monument Hill fault. The Qaf2 and Qaf1 fans along the Monument Hill hanging wall correlate to the two oldest surfaces along the Red Rock hanging wall. The Qaf2 fan is thought to correspond to oxygen isotope stage 6 (130–160 ka), coincident with the Bull Lake glacial maximum (Harkins et al., 2005). Qaf1, in comparison, may represent a single alluvial deposit >160 ka or an amalgamation of older alluvium. A paleosol several meters below the surface indicates Qaf1 materials were deposited on an alluvial or pediment surface of unknown age, and suggests a total alluvial thickness on the order of tens of meters.

### 4.3. Monument Hill fault

The Monument Hill fault system contains three parallel, synthetic, west-dipping fault strands (Fig. 2). The main strand of the fault is 11 km long and extends from Buck Creek in the south to Maurer Creek in the north. It offsets Beaverhead Group conglomerate along its entire length, in contrast to previous mapping by Lonn et al. (2000), which maps Sixmile Creek Formation conglomerate in the footwall. The fault is recognizable by aligned springs, scarps in alluvium, and well-developed facets. The southern tip of this strand is marked by a decrease in facet height, a dominance of Beaverhead Group conglomerate in the hanging wall, and dendritic drainage patterns. The northern tip is marked by captured streams along the projected trace of the fault and a reemergence of Beaverhead and Sixmile Creek conglomerate in the hanging wall. The main strand of the fault is mapped as following a line of bent streams near Maurer Creek, in contrast to published maps which show the fault following the valley-ward limit of bedrock outcrops (e.g. Lonn et al., 2000). The location of the fault was placed along the bent streams based on a lack of well-defined facets at the Sixmile Creek Formation–alluvium contact and geomorphic metrics that support fault activity, as will be discussed later; however, one small splay is mapped along this contact. Timing of most recent rupture along the main strand is poorly constrained by the ages of offset deposits alone, as well-defined scarps occur only in Qaf1 deposits. Length-scaling relationships for normal faults (Schlische et al., 1996) indicate approximately 400 m of cumulative offset along the main strand of the fault (Newton et al., 2005) with uncertainties of up to a hundred meters.

The northwestern and southwestern strands, located valley-ward of the main strand (Fig. 2), offset alluvial deposits and are recognizable by scarps in alluvium, aligned springs, and linear features on aerial photographs. The southwestern fault strand has a strike-length of about 3 km and is recognizable by the presence of scarps near Buck Creek that preserve multiple Quaternary ruptures. Scarp heights in Qaf1 deposits are on average twice as high as scarp heights in Qaf2 deposits (2–7 m and 1–2 m respectively). The northwestern strand, a previously unmapped strand of the Monument Hill fault, has a strike length of about 1.5 km and is recognizable by an offset Qaf2 surface north of Maurer Creek and east of the Clark Canyon Reservoir.

## 5. Fault scarp profile diffusion modeling

Fault scarps that offset alluvium are preserved along all three segments of the Monument Hill fault. The timing of rupture events are bracketed by the age of offset alluvial units and can be estimated from morphologic modeling of scarp degradation derived from topographic profiles of fault scarps (Wallace, 1977; Avouac, 1993; Hanks, 2000). Multiple profiles of scarps along each strand were modeled using two similar, linear diffusion-based approaches (Hanks, 2000, and the SlopeAge modeling program, Nash, 2003). Fault scarp profiles were collected in 2004 using a level and 2-m rod and in 2005 from precision GPS measurements using Trimble 5700 receivers in a post-processed kinematic survey. Multiple profiles by both methods were collected along scarp segments that were assumed to result from a single event. Each profile was oriented perpendicular to the fault scarp and includes the scarp face and adjacent offset fans.

The diffusion models used herein relate scarp age to its topographic profile where scarp slope decreases with time as material from the convex upper slope is removed and deposited on the concave lower slope. This model assumes that the rate of downslope movement of material on the scarp is transport-limited, is proportional to the local gradient, and can be described by linear diffusive processes (Wallace, 1977; Nash, 1980). Single-event, Monument Hill fault scarps are suitable for diffusion modeling as they offset unconsolidated middle to late Pleistocene alluvium derived from a common lithologic source, experience similar climate, and have similar aspect and orientation.

Modeled fault scarp ages were calculated using the following linear diffusion equation (Hanks, 2000),

$$\frac{\mathrm{d}u}{\mathrm{d}x}\Big|_{x=0} - b = (\alpha - b)\mathrm{erf}\left[\frac{(a/(\alpha - b))}{2\sqrt{(KT)}}\right] \quad (1)$$

where $a$ is half of the offset between the projected footwall and hanging wall surfaces, in meters, $b$ is the regional slope or the undisturbed footwall fan slope, $\alpha$ is the initial scarp slope, d$u$/d$x$ is the observed scarp slope, $K$ is the diffusion constant in m$^2$/kyr, and $T$ is time in kyr. The half offset ($a$), regional slope ($b$), and observed scarp slope (d$u$/d$x$) were obtained directly from the measured profile (Fig. 3). An initial scarp slope ($\alpha$) of 35°, representative of the angle of repose of alluvium, was chosen because the initially steep free face of the scarp will degrade to the angle of repose by gravity-driven rather than diffusive processes over a time span that is short relative to the age of the scarp (Wallace, 1977; Bucknam and Anderson, 1979).

A diffusion constant ($K$) was locally calibrated for the Red Rock valley using measured profiles collected from scarps that offset Qft2 along the Red Rock fault and rupture ages determined from $^{14}$C dating of offset surfaces (Harkins et al., 2005) and trenching (Stickney et al., 1987). The diffusion constant ($K$) from Red Rock fault scarps can be applied to modeled scarps on the Monument Hill fault because of proximity, similar fan age, composition, and climatic conditions of formation. The calculated diffusion constant of 1.257 m$^2$/kyr lies within the range of published $K$ values for the Northern Basin and Range (Pierce and Colman, 1986; Nash, 1984).

Using the locally calibrated $K$, scarp ages were modeled for multiple profiles on each fault strand using both Eq. (1) (Hanks, 2000) and the SlopeAge program (Nash, 2003). Eq. (1) was solved for $T$ using constant values for $\alpha$ and $K$. Values for $a$, $b$, and d$u$/d$x$ were calculated for each profile from regression lines constructed through the reduced scarp face and the footwall alluvial surface data. Forward modeling using SlopeAge solved for $T$ based on the criteria of a minimum root mean square fit between modeled and observed profiles. For these models, an initial profile was incrementally degraded with a $\Delta T$ of individual time steps of 20 years for 500 year intervals and a $K$ of 0.001257 m$^2$/year. The model was run five times for each profile with $\alpha$ varied between 30° and 40° as repeated runs indicted the model is most sensitive to variations in initial scarp profile. Mean modeled ages and 1$\sigma$ standard deviations, using results from both modeling techniques, are 31.2 ± 9.8 ka, 28.9 ± 5.7 ka, and 25.7 ± 5.2 ka for the main, southwest, northwest strands of the Monument Hill fault (Fig. 4, Table 2).

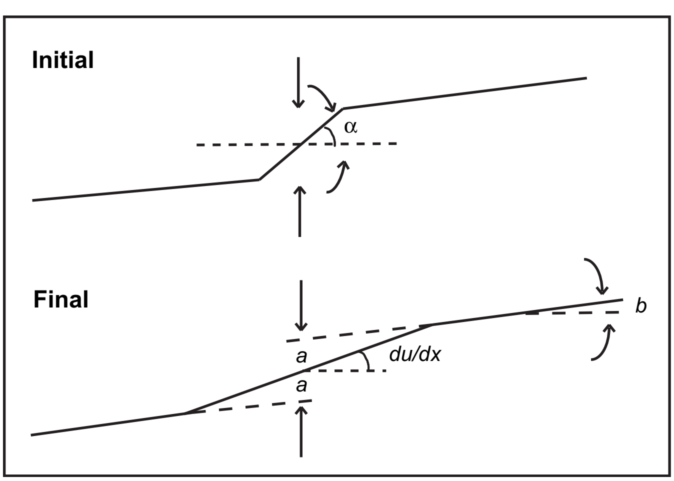


Fig. 3. Idealized initial and final fault scarp profiles for diffusion modeling; measured parameters used in modeling are labeled. Figure adapted from Hanks (2000).

## 6. Geomorphic metrics

Basin metrics were extracted from 30 m US Geological Survey Digital Elevation Models (DEM) and GPS data from a post-processed kinematic survey. The watersheds of 13 2nd- and 3rd-order ephemeral streams transected by the Monument Hill fault were chosen for analysis. Study basins are underlain by the quartzite conglomerate of the Beaverhead Group in their headwaters and alluvium, derived from this bedrock, at their bases. Data from study basins were compared to two control basins, Ashbough Creek and Channel 11, the only tectonically unaltered basins adjacent to the Monument Hill fault with similar underlying lithology, order, orientation, and drainage area to the study basins. Control basins are underlain by the quartzite and limestone conglomerates of the Beaverhead Group, the Sixmile Creek Formation, and the Renova Formation at their headwaters and alluvium derived from this bedrock at their bases (Figs. 2 and 5).

Metrics extracted from 30-m DEM data include basin elongation, hypsometry, and basin slope–area (S-A) plots. Basin elongation (Bull and McFadden, 1977) was measured as the ratio of basin length, parallel to the trunk channel, to average basin width, perpendicular to the trunk channel. Elongate basin geometries are sustained by an uplifting footwall block that drives channel incision and inhibits watersheds from elaboration and widening. Hypsometric plots show the distribution of elevation with respect to area in a watershed, and indicate how well

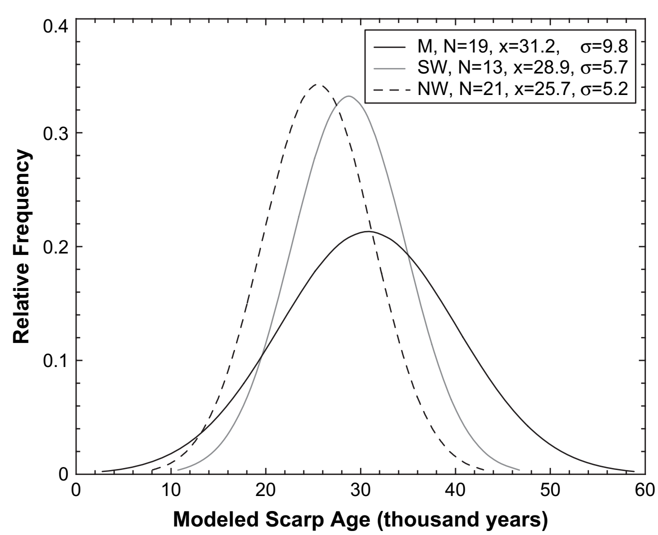


Fig. 4. Synthetic gaussian distributions of modeled fault scarp ages, obtained from the two diffusion modeling techniques discussed in the text, for profiles along the main (M), northwest (NW), and southwest (SW) strands of the Monument Hill fault. Curves are derived from the arithmetic mean ($x$) and standard deviation ($\sigma$) for $N$ ages, calculated using the $N-1$ method; ages and $KT$ values are listed in Table 2. Note the overlap in 1$\sigma$ between the three strands, and that modeled ages from all three strands cluster between 22 and 32 ka. A $t$-test does not distinguish between the mean modeled ages of most recent rupture for the two valley-ward strands.

Table 2
Modeled *KT* values and ages for single-event fault scarp profiles along the main, southwest, and northwest strands of the Monument Hill fault

| Profile name | Offset surface | Modeled *KT* ($m^2$)[a] | Modeled *KT* ($m^2$)[b] | Modeled ages (ka)[a] | Modeled ages (ka) |
|---|---|---|---|---|---|
| M1[c] | $Qf_1$ | 41.0 | 53.4, 40.2, 41.5, 59.1, 45.9 | 32.6 | 42.5, 32.0, 33.0, 47.0, 36.5 |
| M2[d] | $Qf_1$ | 15.7 | 28.9, 25.8, 25.8, 30.2, 27.0 | 12.5 | 23.0, 20.5, 20.5, 24.0, 21.5 |
| M3[c] | $Qf_1$ | 30.2 | 56.6, 56.6, 42.7, 49.7, 40.9 | 24.0 | 45.0, 45.0, 34.0, 39.5, 32.5 |
| M4[c] | $Qf_1$ | 34.5 | – | 27.4 | – |
| SW1[c] | $Qf_2$ | 32.4 | – | 25.8 | – |
| SW2[c] | $Qf_2$ | 20.5 | 32.7, 40.2, 42.1, 40.2, 39.0 | 16.3 | 26.0, 32.0, 33.5, 32.0, 31.0 |
| SW3[d] | $Qf_2$ | 37.5 | 26.4, 46.5, 34.6, 44.0, 36.5 | 29.9 | 21.0, 37.0, 27.5, 35.0, 29.0 |
| NW1[c] | $Qf_2$ | 22.5 | – | 17.9 | – |
| NW2[c] | $Qf_2$ | 43.3 | 41.5, 33.3, 37.7, 38.3, 36.5 | 34.5 | 33.0, 26.5, 30.0, 30.5, 29.0 |
| NW3[d] | $Qf_2$ | 35.0 | – | 27.8 | – |
| NW4[c] | $Qf_2$ | 35.7 | – | 28.4 | – |
| NW5[d] | $Qf_2$ | 26.2 | 41.5, 33.3, 37.7, 25.1, 23.9 | 20.9 | 33.0, 26.5, 30.0, 20.0, 19.0 |
| NW6[d] | $Qf_2$ | 25.1 | 25.1, 25.8, 27.0, 27.0, 26.4 | 27.3 | 20.0, 20.5, 21.5, 21.5, 21.0 |

Modeled ages calculated with a locally calibrated *K* of 1.257 $m^3$/kyr. See Fig. 2 for profile locations.
[a] Calculations made using the method outlined in Hanks (2000).
[b] Calculations made using the SlopeAge program (Nash, 2003).
[c] Topographic scarp profiles collected with GPS.
[d] Topographic scarp profiles collected with a 2-m rod.

hillslopes and uplands are graded to the main channels (Strahler, 1952). Basin hypsometries were compared based on the shape of hypsometric curves and calculations of hypsometric integrals (Pike and Wilson, 1971). When channel profiles are plotted in logarithmic slope–area space, segments of differing steepness and concavity can be identified, assuming channel slope and upstream drainage area are related by a power law, as described for detachment-limited bedrock channels (e.g. Hack, 1973; Flint, 1974; Howard and Kerby, 1983; Whipple, 2004). Channel slope–basin area plots take advantage of the inverse relation between channel slope and discharge and can be used to identify anomalously steep channel segments (e.g. Snyder et al., 2000).

Metrics obtained from GPS measurements include channel long profiles and slope–length indices (SL index). GPS data were collected for channels 2, 4, 5, 6, 7, 8, 10, 11, Maurer Creek and Buck Creek (Fig. 5) in a post-processed kinematic survey with a five-second sample interval. Long profile data were smoothed by a loess regression and channel elevation was plotted as a function of distance from the source. Long profiles were used as a first-order assessment of channel form to identify disruptions to the smooth, concave profile expected for an equilibrated stream. Changes in channel slope were quantified by calculation of the SL index, the product of channel slope and downstream distance for a point in the channel profile (Hack, 1973). Slope–length indices were calculated from long profile data by multiplying channel slope, calculated over a five-point moving window, by distance from the source. Local peaks in SL indices are associated

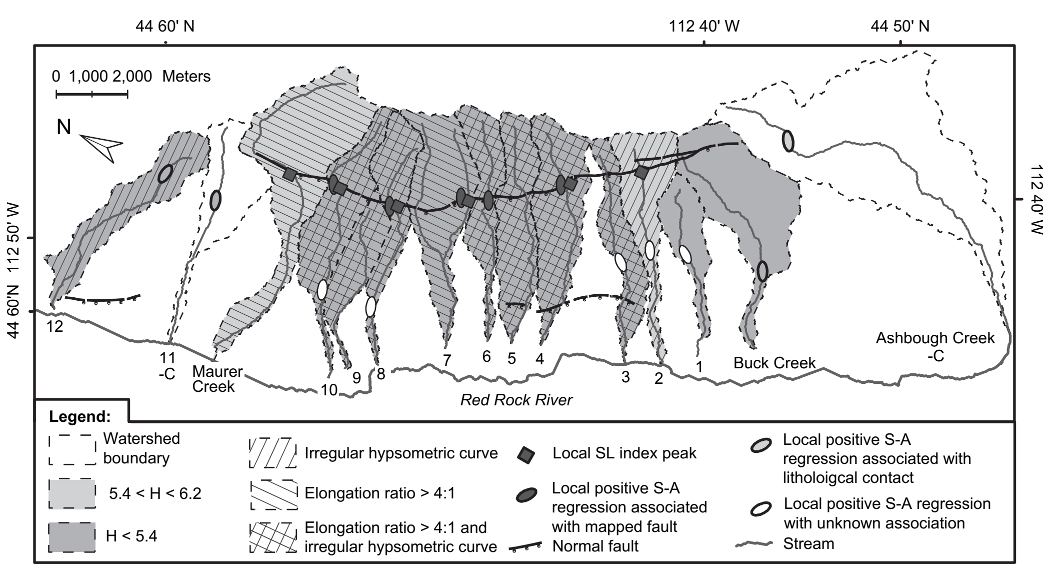


Fig. 5. Summary of basin metrics. Control basins marked by -C. Watersheds transected by the Monument Hill fault are elongate, display irregular hypsometric plots, and have hypsometric integrals ($H$) less than that of control basins. Channel segments with anomalously high slopes, noted by local SL index peaks and positive S-A regressions, are aligned with the mapped position of the main strand of the fault. See Fig. 1 for location.

with anomalously steep portions of the channel of either lithologic or tectonic origin.

Watersheds that transect the Monument Hill fault are elongate, have irregular hypsometries not consistent with a basin with an equal distribution of elevation, low hypsometric integrals, and oversteepened segments in the trunk channel coincident with the mapped fault trace (Figs. 5 and 6; Table 3). Conversely, watersheds not transected by the Monument Hill fault are less elongate, have hypsometries consistent with basins with an equal distribution of elevation, higher hypsometric integrals, and oversteepened segments coincident with lithologic contacts only. Drainage basins that are transected by the main strand of the Monument Hill fault generally have aspect ratios greater than 4.0, while control basins have aspect ratios less than 4.0 (Table 3). Hypsometric curves for basins transected by the fault deviate from the concave-convex pattern expected for a channel in equilibrium, and do not show a dominance of area at mid-elevations (Fig. 6).

Local peaks in SL indices are present in nearly all of the studied basins (Fig. 5). Several channels display SL index peaks where the channel crosses from the footwall to the hanging wall of the Monument Hill fault. Similarly, when channel profiles are plotted in slope–area space, several channels display segments with a positive regression that correspond to the Monument Hill fault (Fig. 5). However, oversteepened channel segments are also present where the channel cuts through a more resistant lithology, such as the limestone conglomerate of the Beaverhead Group and the volcanic beds of the Renova and Sixmile Creek formations, as well as in locations not associated with an active fault strand or a resistant lithology (Figs. 2 and 5). The rock-type controlled channel segments are easily distinguished from potential tectonic influences by the well-known, mapped distribution of rock types in the study area.

## 7. Discussion

New geologic mapping, morphologic modeling, and geomorphic metrics have improved the characterization the Monument Hill fault and collectively support the interpretation of a youthful, active fault system. This interpretation is consistent with the fault's limited strike length, exposures of bedrock in the hanging wall, a thin alluvial fill, and the lack of a prominent range front along the Red Rock Hills (Fig. 2). It is also consistent with geologic observations and interpretations for the Red Rock fault, which has a ~1 Ma

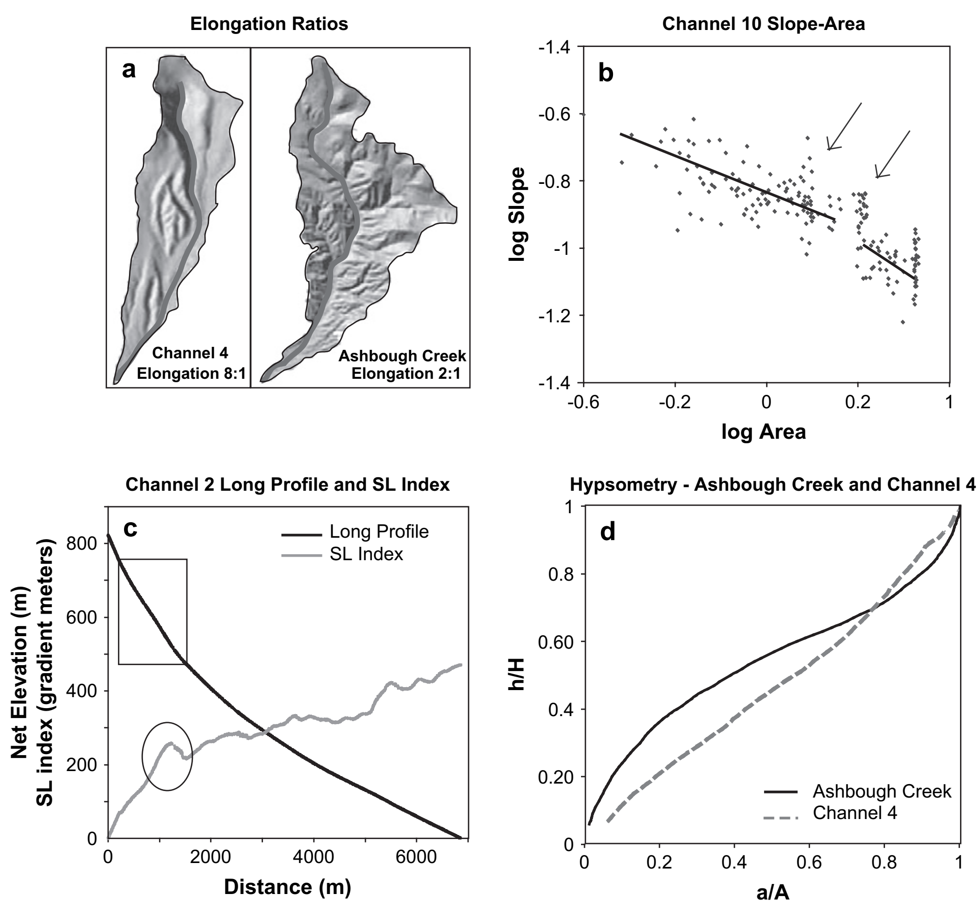


Fig. 6. Examples of geomorphic metrics for basins in the Red Rock Hills. (a) Elongation ratios of basins transected by the Monument Hill fault (Channel 4) are significantly greater than those of control basins (Ashbough Creek). (b) When modeled in slope–area space, channels in tectonically altered basins have segments with positive regressions (arrows), indicating oversteepened channel segments. (c) Channels in tectonically altered basins contain perturbations in their long profiles (box) that correspond with peaks in SL index (oval). (d) Hypsometric curves for tectonically altered basins (Channel 4) deviate from the concave-convex pattern seen in control basins (Ashbough Creek), and lack a dominance of area at mid-elevations.

Table 3
Hypsometric integrals ($H$) and elongation ratios for two control basins and thirteen tectonically altered basins (see Fig. 5 for basin locations)

| Watershed name | Hypsometric integral ($H$) | Elongation ratio |
|---|---|---|
| Ashbough Creek[a] | 0.54 | 2.1 |
| Ch11[a] | 0.61 | 3.8 |
| Ch12 | 0.45 | 6.7 |
| Maurer Creek | 0.54 | 3.5 |
| Channel 10 | 0.44 | 6.0 |
| Channel 9 | 0.46 | 4.9 |
| Channel 8 | 0.53 | 5.8 |
| Channel 7 | 0.51 | 3.7 |
| Channel 6 | 0.53 | 7.9 |
| Channel 5 | 0.46 | 5.7 |
| Channel 4 | 0.49 | 4.3 |
| Channel 3 | 0.38 | 7.5 |
| Channel 2 | 0.55 | 4.2 |
| Channel 1 | 0.53 | 3.7 |
| Buck Creek | 0.51 | 2.3 |

[a] Control basin.

history of activity consistent with a 1 mm/year slip rate and inferred 1 km of total offset (Harkins et al., 2005). A total offset of 400 m for the Monument Hill fault, inferred from length–scaling relationships, is consistent with a northward decrease in displacement along the Red Rock fault evident from entrenchment of young fans (Harkins et al., 2005) and low slip rates along the northern segment (Stickney, 2000). This interpretation supports a northward decrease in total extension across the Red Rock Valley.

Based on new mapping and cross sections, the positions of the Monument Hill fault and other extensional structures in the Red Rock Valley are interpreted to be controlled largely by the location of frontal Sevier thrust sheets. While the Red Rock fault parallels the Tendoy thrust sheet, the Monument Hill fault parallels the front of the McKenzie thrust system, which crops out 3–4 miles farther into the foreland than the Tendoy sheet (Fig. 7). The accommodation zone at Kidd is located where Tendoy thrust sheet shortening is laterally transferred to displacement within the McKenzie thrust system. It is probable that the position of the Kidd accommodation zone is controlled by the location of this older, contractional, transfer zone.

The Monument Hill fault includes an 11 km main strand and two synthetic 1–3 km long strands that are not joined by surface ruptures. Although previous maps trace the southwestern fault strand toward the north following a line of springs, the two basinward strands are not connected at the surface by any recognized scarps. Based on new mapping (Regalla et al., 2006), these springs are re-interpreted to mark the location at depth where groundwater flowing through the poorly indurated quartzite conglomerate of the Beaverhead Group surfaces after encountering the well-indurated limestone conglomerate of the Beaverhead Group and underlying Paleozoic

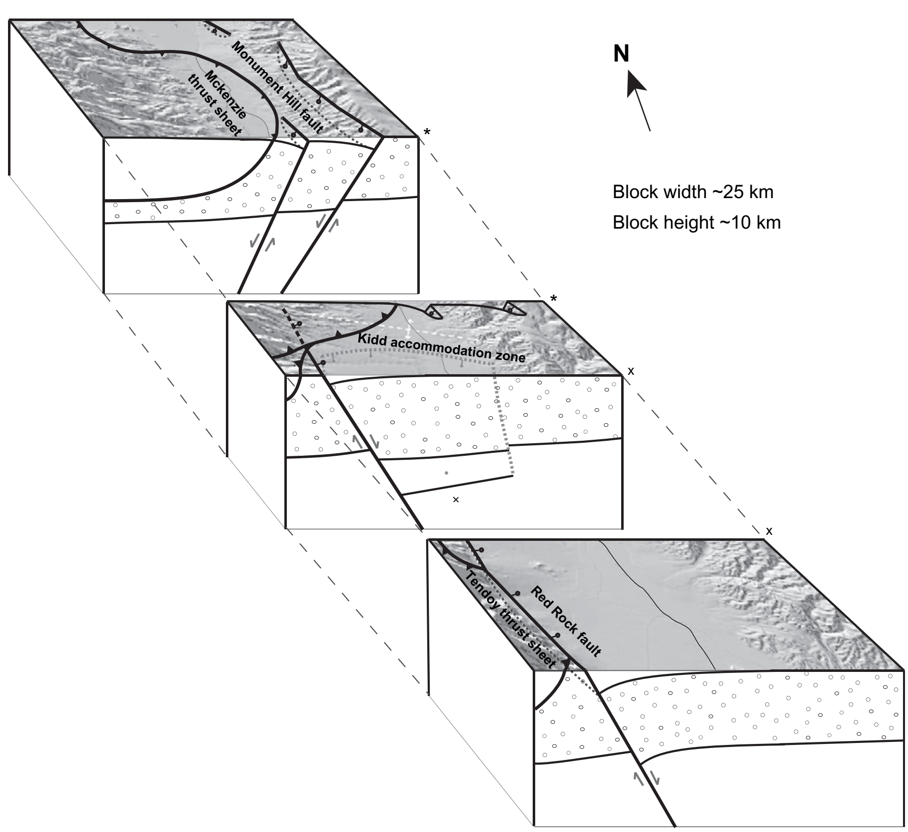


Fig. 7. Schematic diagram of the Red Rock Valley showing the proposed geometry of the Monument Hill fault, Red Rock fault, and Kidd accommodation zone and their relationship to Sevier structures. Simplified cross-sections on block faces based on previously published maps (Harkins et al., 2004; Aschoff and Schmitt, 2004; Regalla et al, 2006). Stars and crosses indicate matching block edges.

carbonates. If the southwestern and northwestern strands of the Monument Hill fault are linked at depth, no surface rupture was generated along this connecting portion of the fault since the deposition of Qaf1 deposits >160 ka. This new interpretation substantially reduces the length of the southwestern strand.

Fault scarps that offset multiple alluvial surfaces have greater total offsets in older alluvial units, indicating that the Monument Hill fault has ruptured multiple times in the Pleistocene. It is inferred from comparative scarp heights of single event scarps in Qaf2 fans and multiple event scarps in Qaf1 fans that a single rupture event produces ~1 m of offset on the basinward strands of the Monument Hill fault and ~3.5 m of offset on the main strand of the Monument Hill fault. Ruptures having these maximum displacements are associated with earthquakes of M 6.0–6.7, based on scaling relationships (Wells and Coppersmith, 1994). This interpretation may represent a minimum magnitude range necessary to produce surface rupture along extensional faults in this region of southwestern Montana, as recent local earthquakes have had maximum magnitudes of up to M 5.6 without forming a surface rupture.

### 7.1. Topographic metrics

The Quaternary activity of the Monument Hill fault system is reflected in basin and channel morphologies (Figs. 5 and 6). Oversteepened channel segments indicated by slope–length index peaks and positive correlations between slope and area are consistently located along the mapped trace of the main strand of the Monument Hill fault system (Fig. 5), implying recent rupture along this strand of the fault or cementation of the fault zone. A knick zone, however, is not observed in every channel, and no recognizable offset is seen in Qaf3 surfaces. These seemingly contradictory data may be explained if the channels were offset during the Late Pleistocene followed by minimal upstream migration of the knick zone, then subsequently filled with Qaf3 deposits that have been incompletely exhumed during the Holocene. The paucity of water in these ephemeral channels could lead to slow migration of the knick zone away from the scarp, explaining the position of the modern knick zone within meters of the rupture, and could result in the incomplete exhumation of the knick zone, as is observed in some channels.

Other oversteepened channel segments indicated by positive correlations between slope and basin area are not coincident with the mapped fault trace (Fig. 5). These points in Ashbough Creek, Buck Creek, and channels 11 and 12 are the result of local outcrops of resistant lithologies, including volcanic rocks and limestone conglomerate. Other areas of high channel slope located between Buck Creek and Maurer Creek cannot be explained by resistant lithologies and may indicate regions deformed along fault segments with no single, discrete surface rupture.

Basins transected by the main strand of the fault are elongate and have hypsometries that reflect both the high footwall elevations and graded alluvial surfaces sloping down to valley bottom. These characteristics are interpreted to reflect sustained footwall uplift, channel incision, and deposition of alluvium on the hanging wall of the Monument Hill fault. While the basin metrics of hypsometry and elongation alone do not definitively indicate tectonic activity, due to the range of variability among basins, the general patterns are consistent with this interpretation and do not contradict data from other metrics.

### 7.2. Kinematics of Monument Hill fault

The long-term, integrated record of climate, sedimentation, and tectonic activity are reflected in the planimetric distribution of alluvial surfaces (Bull, 1961, 1984; Denny, 1967) along the Monument Hill fault. Because factors such as climate and bedrock lithology are relatively constant within the study area, along strike variations in inset and burial patterns are most controlled by variations in tectonic activity and individual basin sediment loads. Incision and burial patterns are controlled by activity along the main strand of the Monument Hill fault but may be locally perturbed by activity along the southwestern and northwestern strands.

The change in depositional pattern from inset Qaf3 channels along the southern fault extent to wide Qaf3 fans along the northern fault extent is coincident with the location where the main strand of the Monument Hill fault turns north and cuts into the high standing topography of the Red Rock Hills (Figs. 1 and 2). These depositional changes are interpreted to be the result of a change in the sense of slip along the main strand of the Monument Hill fault from predominantly dip slip in the south to oblique normal displacement with a component of left-lateral slip in the north. This would result in a decrease in cumulative down-dip offset along the northern portion of the fault, limiting the space available for sediment accumulation adjacent to the fault, and would increase the sediment load supplied by ephemeral streams flowing along easily erodible fault rocks for hundreds of meters before cutting back into the Red Rock Hills. The shift in fault kinematics from dip slip to oblique slip along the northern portion of the main strand of the Monument Hill fault is consistent with observations that indicate a shift in kinematics along faults in relay zones from dip slip to oblique slip in the zone of overlap between adjacent faults in the stages prior to fault linkage (Acocella et al., 2000).

The kinematics of the Monument Hill fault are consistent with extension directions in the Red Rock Valley and broader Basin and Range Province in southwestern Montana. The dominant dip slip motion on the Monument Hill fault is consistent with northeast-southwest regional extensional directions obtained from previous fault characterizations (Harkins et al., 2005) and geologic indicators (Zoback and Zoback, 1989) (Fig. 1). The inferred component of strike slip movement on the northern portion of the Monument Hill fault and the overall curved geometry of the Red Rock Valley are consistent with north-south to northeast-southwest extensional directions derived from focal mechanisms (Stickney and Lageson, 2002) and a fractured clast study (Hurlow, 1995) (Fig. 1). Both support a component of left-lateral transtension necessary to accommodate north-northeast south-southwest extension in the curved Red Rock Valley.

### 7.3. Clustering along the Monument Hill fault

The ages of offset surfaces and corresponding scarp heights indicate at least two rupture events along the Monument Hill fault in the Pleistocene and are consistent with a clustering of related events on multiple strands of the fault. All three strands have scarps that offset Qaf2 surfaces but do not offset Qaf3 surfaces, and have modeled ages that cluster around 22–32 ka (Fig. 4, Table 2). These data are interpreted to represent a clustering of related events that occurred between 22 and 32 ka along the three strands of the Monument Hill fault. The main and southwestern strands also preserve a record of at least one additional, older rupture event. Both strands contain scarps that offset only Qaf1 deposits, which have approximately twice as much offset as Qaf2 deposits. Because these scarps are the result of multiple events, they were not modeled, but the age of the offset Qaf1 surface places the ruptures >160 ka. Similarities in the ages of offset surfaces and in scarp geometries between the two ruptures suggest that they may also be the result of a spatial clustering of related events. It is possible that this older rupture also occurred along the northwestern strand but is not recorded due to a lack of Qaf1 deposits. Rupture ages of a greater resolution are necessary to test this interpretation.

Evidence for a clustering of events on multiple strands of the Monument Hill fault suggests non-steady recurrence intervals. Similar patterns in clustering have been found on nearby Basin and Range faults, including the Lemhi (Hemphill-Haley et al., 1994; Knuepfer, 1994) and the Lost River faults (Olig et al., 1994, 1995) for which paleoseismic records suggest non-steady rupture behavior with several large ruptures occurring within hundreds to thousands of years, separated by tectonically quiet intervals of tens of thousands of years. Similarities exist between the timing of clustered events on the Monument Hill and Lost River faults. Events appear clustered on the Monument Hill fault 22–32 ka and >160 ka and on the Lost River fault at $20 \pm 4$ ka and 140–220 ka (Olig et al., 1995, 2002). Although speculative, correlations between the timing of clustered events on these two fault systems may suggest potential for regional correlations of events in the northern Basin and Range.

### 7.4. Geometry of the Red Rock Valley

The Monument Hill and Red Rock faults are viewed as a single extensional system connected by a mid-basin accommodation zone at Kidd that accommodates a reverse in fault polarity across the Red Rock Valley (Figs. 1 and 7). Whereas young fans bury older deposits along the northern Monument Hill fault and the southern segments of the Red Rock fault, young fans become progressively more inset toward the Kidd accommodation zone (Fig. 2; Harkins et al., 2005; Stickney and Lageson, 2002). The valleyward progradation of fans at Kidd reflects a lack of accommodation space adjacent to the graben-bounding faults resulting from a decrease in offset along the Monument Hill and Red Rock faults in the area of overlap between the two faults.

The geometry and spacing of the oppositely dipping Monument Hill and Red Rock faults are consistent with a transfer of extensional strain across an anticlinal accommodation zone—one formed in the overlap between two antithetic half grabens—whose axis trends at an oblique angle to the main graben-bounding faults (e.g. Morley et al., 1990; Faulds and Varga, 1998) (Figs. 1 and 7). The trend of the axis is roughly coincident with the strike of the south-southwest-dipping nodal plane of the 1999 Red Rock Valley earthquake (Stickney and Lageson, 2002) (Fig. 1). Fault plane solutions for the Red Rock Valley earthquake show almost pure dip slip with a minor component of sinistral slip on a fault within the Kidd accommodation zone (Stickney and Lageson, 2002). The kinematics of this rupture necessitates the presence of a south-southwest dipping fault (Stickney and Lageson, 2002) that roughly parallels the axis of the accommodation zone. This fault, or system of faults, are interpreted to open in a scissor-like manner toward the Red Rock fault in order to accommodate left lateral slip and an increase in the magnitude of extension in the southern portion of the Red Rock Valley.

Extension across the Red Rock Valley is accommodated along both the Red Rock and Monument Hill faults in a system where slip is transferred from the Red Rock fault to the Monument Hill fault across the Kidd accommodation zone. However, the two fault systems are not seismogenically linked. This interpretation is supported by the unique rupture histories of the Monument Hill and Red Rock faults (this study; Harkins et al., 2005), and the accommodation zone at Kidd may be currently acting as a rupture barrier (Fonseca, 1988; Gawthorpe and Hurst, 1993) between these two fault systems.

## 8. Conclusions

Characterization of the Monument Hill fault has been refined by 1:24,000-scale mapping of bedrock and surficial geology, diffusion modeling of fault scarps, and analysis of topographic metrics. The Monument Hill fault system consists of an 11 km long main strand that extends from Buck Creek to Maurer Creek, a 3 km long southwestern strand near Buck Creek, and a 1.5 km long strand near Maurer Creek and the Clark Canyon Dam. Length-scaling relationships indicate ~400 m cumulative displacement along the main strand of the fault, and scarp geometries indicate total Pleistocene displacements along the lower strands of 2–7 m. Fault scarp heights indicate that a single rupture event produces ~1 m of slip on the basinward strands of the Monument Hill fault and ~3.5 m of slip on the main strand and are likely the product of magnitude 6.0–6.7 earthquakes. The positions of the Monument Hill and Red Rock faults and the Kidd accommodation zone are patterned after Sevier-age structural geometries along the thrust front.

Results from mapping and morphologic scarp modeling are consistent with a clustering of rupture events along the Monument Hill fault system 22–32 ka and potentially related events >160 ka. Clustered events and surface rupture geometries for the Monument Hill fault are consistent with models that support communication between fault strands where slip along one strand triggers slip on adjacent strands. Clustering of paleoseismic events has been observed on several faults in the northern Basin and Range Province and may indicate a non-uniform recurrence interval for the Monument Hill fault.

Recent activity along the Monument Hill fault is supported by geomorphic metrics, which indicate elongate basin geometries sustained by continued footwall uplift and oversteepened channel segments resulting from recent offset of the main fault strand or a cementation of the fault zone. Field and geomorphic evidence for partially exhumed knick zones along the main strand of the Monument Hill fault are consistent with a late Pleistocene rupture, burial by latest Pleistocene alluvium, and Holocene exhumation.

The planimetric distribution of alluvial fans and change in fault trace geometry indicate a change in kinematics along the strike of the main strand Monument Hill fault system, from dip slip in the south to dip slip with a component of left-lateral slip in the north. This kinematic shift is consistent with observations made for faults in relay zones during the stages prior to fault linkage. The transition in depositional pattern in young alluvial surfaces from burial along the Monument Hill fault and Red Rock fault to inset channels near the Kidd accommodation zone is consistent with a lack of accommodation space resulting from a decrease in total slip along the overlapping portions of the faults.

The surface rupture patterns of the Monument Hill and Red Rock faults and fault plane solutions from the 1999 Red Rock Valley earthquake are consistent with an anticlinal accommodation zone in the Red Rock Valley containing a south-southwest dipping fault that has produced no surface rupture in the Quaternary and that is oriented roughly parallel to the axis of the extensional anticline. This zone accommodates a change in polarity across the Red Rock Valley, with a decrease in extension from the southern to the northern Red Rock Valley, and may be acting as a rupture barrier between the Monument Hill and Red Rock faults. The active tectonics of the Red Rock Valley may represent the youthful stages of graben evolution in the Basin and Range Province north of the Snake River Plain.

## Acknowledgements

Funding for this project was provided by EDMAP Program of the National Cooperative Geologic Mapping Program of the US Geological Survey under Contract Numbers 05HQAG0015 and 04HQAG0099. A special thanks to editor William Dunne, reviewer David Lageson and especially reviewer Christopher Menges for their comments which improved the clarity of the manuscript, Karen Porter and the reviewers at the Montana Bureau of Mines and geology for suggestions and edits to the geologic map, UNAVCO for providing GPS equipment, Jim Greenburg for assistance with GPS equipment and data processing, Daryn Reyman and Michael Newton for field assistance, Nathan Harkins for fault scarp profile data, and Danny and Kristen Johnson for hospitality and land access permissions for two field seasons. The following programs were used in this study: ArcGIS, Trimble Geometrics Office, and SlopeAge.

## References

Acocella, V., Gudmundsson, A., Funiciello, R., 2000. Interaction and linkage of extension fractures and normal faults; examples from the rift zone of Iceland. Journal of Structural Geology 22, 1233–1246.

Acocella, V., Morvillo, P., Funiciello, R., 2005. What controls relay ramps and transfer faults within rift zones? Insights from analogue models. Journal of Structural Geology 27, 397–408.

Anders, M.H., Geissman, J.W., Piety, L.A., Sullivan, J.T., 1989. Parabolic distribution of circum-eastern Snake River Plain seismicity and latest Quaternary faulting; migratory pattern and association with the Yellowstone hot spot. Journal of Geophysical Research 95, 1589–1621.

Anderson, L.W., Piety, L.A., Olig, S.S., Forman, S.L., 2003. Late Quaternary activity of the Canyon Ferry Fault, Montana. Geological Society of America Abstracts with Programs 35, 11.

Aschoff, J.L., Schmitt, J.G., 2004. Geologic Map of the Dell 7.5-minute Quadrangle, Cordilleran Fold and Thrust Belt, Southwest Montana. Montana Bureau of Mines and Geology Open File Report 520, scale 1:24, 000, 33 pp.

Avouac, J.P., 1993. Analysis of scarp profiles; evaluation of errors in morphologic dating. Journal of Geophysical Research, B. Solid Earth and Planets 98, 6745–6754.

Bartholomew, M.J., Stickney, M.C., Wasklewicz, T.A., 2002. Interaction between the northern Basin and Range and the Yellowstone stress fields near the Red Rock Fault, southwestern Montana. Geological Society of America Abstracts with Programs 36, 12.

Birkeland, P.W., 1999. Soils and Geomorphology. Oxford University Press, New York.

Bucknam, R.C., Anderson, R.E., 1979. Estimation of fault scarp ages from a scarp-height-slope-angle relationship. Geology 7, 11–14.

Bull, W.B., 1961. Tectonic significance of radial profiles of alluvial fans in western Fresno County. Article 75. US Geological Survey Professional Paper, California, pp. B182–B184.

Bull, W.B., 1984. Tectonic geomorphology. Journal of Geological Education 31, 310–324.

Bull, W.B., McFadden, L.D., 1977. Tectonic Geomorphology North and South of the Garlock Fault, California. A Proceedings Volume of the Annual Geomorphology Symposia Series 8, 115–138.

Chery, J., Carretier, S., Ritz, J.F., 2001a. Postseismic stress transfer explains time clustering of large earthquakes in Mongolia. Earth and Planetary Science Letters 194, 277–286.

Chery, J., Merkel, S., Bouissou, S., 2001b. A physical basis for time clustering of large earthquakes. Bulletin of the Seismological Society of America 91, 1685–1693.

Dawers, N.H., Anders, M.H., 1995. Displacement-length scaling and fault linkage. Journal of Structural Geology 17, 607–614.

Denny, C.S., 1967. Fans and pediments. American Journal of Science 265, 81–105.

Di Bucci, D., Massa, B., Zuppetta, A., 2006. Relay ramps in active normal fault zones; a clue to the identification of seismogenic sources (1688 Sannio earthquake, Italy). Geological Society of America Bulletin 118, 430–448.

Faulds, J.E., Varga, R.J., 1998. The role of accommodation zones and transfer zones in the regional segmentation of extensional terranes. In: Faulds, J.E., Stewart, J.H. (Eds.), Accommodation Zones and Transfer Zones: the Segmentation of the Basin and Range Province. Geological Society of America Special Paper, 323. Geological Society of America, Boulder, CO.

Fields, R.W., Rasmussen, D.L., Tabrum, A.R., Nichols, R., 1985. Cenozoic rocks of the Intermontane basins of western Montana and eastern Idaho: a summary. In: Flores, R.M., Kaplan, S.S. (Eds.), Cenozoic Paleogeography of the West-Central United States. Rocky Mountain Paleogeography Symposium, 3, pp. 9–36.

Flint, J.J., 1974. Stream gradient as a function of order, magnitude, and discharge. Water Resources Research 10, 969–973.

Fonseca, J., 1988. The Sou Hills; a barrier to faulting in the central Nevada seismic belt. Journal of Geophysical Research 93, 475–489.

Fritz, W.J., Sears, J.W., 1993. Tectonics of the Yellowstone hotspot wake in southwestern Montana. Geology 21, 427–430.

Gawthorpe, R.L., Hurst, J.M., 1993. Transfer zones in extensional basins; their structural style and influence on drainage development and stratigraphy. Journal of the Geological Society of London 150, 1137–1152.

Gibbs, A.D., 1984. Structural evolution of extensional basin margins. Journal of the Geological Society of London 141, 609–620.

Gile, L.H., Peterson, F.F., Grossman, R.B., 1966. Morphological and genetic sequences carbonate accumulation in desert soils. Soil Science 101, 347–360.

Greenwell, R.A., 1997. Alluvial fan development, the key to segmentation of the Red Rock fault, Southwestern Montana. MS thesis. University of South Carolina.

Hack, J.T., 1973. Stream-profile analysis and stream-gradient index. Journal of Research of the US Geological Survey 1, 421–429.

Haley, J.C., Perry, W.J., 1991. The Red Butte Conglomerate – a thrust-belt derived conglomerate of the Beaverhead Group, Southwestern Montana. US Geological Survey Bulletin 1945.

Haller, K.M., 1988. Segmentation of the Lemhi and Beaverhead faults, east-central Idaho, and Red Rock fault, southwestern Montana, during the late quaternary. PhD dissertation. University of Colorado.

Haller, K.M. (compiler), 1993. Fault number 648a, Red Rock Hills fault, Monument Hill section, in: Quaternary Fault and Fold Database of the United States. US Geological website, http://earthquakes.usgs.gov/regional/qfaults, accessed on 05/16/2006.

Hanks, T.C., 2000. The age of scarplike landforms from diffusion-equation analysis, in: Quaternary Geochronology: Methods and Applications, pp. 313–338.

Harkins, N.W., Anastasio, D.J., Pazzaglia, F.J., 2005. Tectonic geomorphology of the Red Rock fault, insights into segmentation and landscape evolution of a developing range front normal fault. Journal of Structural Geology 27, 1925–1939.

Harkins, N.W., Latta, D.K., Anastasio, D.J., Pazzaglia, F.J., 2004. Surficial and bedrock geologic map of the Dixon Mountain 7.5′ Quadrangle, Southwest Montana. Montana Bureau of Mines and Geology Open File Report 495, scale 1:24, 000, 12 pp.

Hemphill-Haley, M.A., Sawyer, T.L., Knuepfer, P.L.K., Forman, S.L., Wong, I.G., 1994. Late Quaternary paleoseismicity and segmentation along the southern Lemhi Fault, southeastern Idaho. In: Prentice, C.S., Schwartz, D.P., Yeats, R.S. (Eds.), Proceedings of the Workshop on Paleoseismology. US Geological Survey Open File Report, pp. 81–83.

Howard, A.D., Kerby, G., 1983. Channel changes in badlands. Geological Society of America Bulletin 94, 739–752.

Hurlow, H.A., 1995. Pliocene or younger paleostress directions from fractured clasts, Sixmile Creek Formation, Lower Red Rock Valley, southwestern Montana. In: Mogk, D.W. (Ed.), Field Guide to Geologic Excursions in Southwest Montana. Northwest Geology, Vol. 24, pp. 229–236.

Hus, R., Acocella, V., Funiciello, R., De Batist, M., 2005. Sandbox models of relay ramp structure and evolution. Journal of Structural Geology 27, 459–473.

Janecke, S.U., Skipp, B., Perry Jr., W.J., 2002. Out-of-sequence and folded short thrusts produced by protracted forland-thrust-belt interactions. SW Montana. Geological Society of America Abstracts with Programs 36, 77.

Johnson, P.P., 1981. Geology along the Red Rock Fault and Adjacent Red Rock Basin, Beaverhead County, Montana. Montana Geological Society 1981 Field Conference, SW Montana, pp. 245–251.

Kenner, S.J., Simons, M., 2005. Temporal clustering of major earthquakes along individual faults due to post-seismic reloading. Geophysical Journal International 160, 179–194.

King, G.C.P., Stein, R.S., Lin, J., 1994. Static stress changes and the triggering of earthquakes. Bulletin of the Seismological Society of America 84, 935–953.

Knuepfer, P.L.K., 1994. Implications for the nature of rupture segmentation from paleoseismic studies of normal faults, east-central Idaho. In: Prentice, C.S., Schwartz, D.P., Yeats, R.S. (Eds.), Proceedings of the Workshop on Paleoseismology. US Geological Survey Open File Report, pp. 97–99.

Kuenzi, W.D., Fields, R.W., 1971. Tertiary stratigraphy, structure, and geologic history, Jefferson Basin, Montana. Geological Society of America Bulletin 82, 3373–3394.

Jackson, C.A.L., Gawthorpe, R.L., Sharp, I.R., 2002. Growth and linkage of the East Tanka fault zone, Suez Rift; structural style and syn-rift stratigraphic response. Journal of the Geological Society of London 159, 175–187.

Lonn, J.D., Skipp, B., Ruppel, E.T., Janecke, S.U., Perry, W.J., Sears, J.W., Bartholomew, M.J., Stickney, M.C., Fritz, W.J., Hurlow, H.A., Thomas, R.C., 2000. Geologic Map of the Lima 30′ × 60′ Quadrangle, Southwest Montana. Montana Bureau of Mines and Geology Open File 408, scale 1:100,000.

Lynch, J.C., Burgmann, R., Richards, M.A., Ferencz, R.M., 2003. When faults communicate; viscoelastic coupling and earthquake clustering in a simple two-fault system. Geophysical Research Letters 30, 1–4.

Marco, S., Stein, M., Agnon, A., Ron, H., 1996. Long-term earthquake clustering; a 50,000-year paleoseismic record in the Dead Sea Graben. Journal of Geophysical Research 101, 6179–6191.

McDowell, R.J., 1997. Evidence for synchronous thin-skinned and basement deformation in the Cordilleran fold-thrust belt: the Tendoy Mountains, southwestern Montana. Journal of Structural Geology 19, 77–87.

McLeod, A.E., Dawers, N.H., Underhill, J.R., 2000. The propagation and linkage of normal faults; insights from the Strathspey-Brent-Statfjord fault array, northern North Sea. Basin Research 12, 263–284.

Morley, C.K., 1999. Patterns of displacement along large normal faults; implications for basin evolution and fault propagation, based on examples from East Africa. AAPG Bulletin 83, 613–634.

Morley, C.K., Nelson, R.A., Patton, T.L., Munn, S.G., 1990. Transfer zones in the East African Rift system and their relevance to hydrocarbon exploration in rifts. AAPG Bulletin 74, 1234–1253.

Nash, D.B., 1980. Morphologic dating of degraded normal fault scarps. Journal of Geology 88, 353–360.

Nash, D.B., 1984. Morphologic dating of fluvial terrace scarps and fault scarps near West Yellowstone, Montana. Geological Society of America Bulletin 95, 1413–1424.

Nash, D.B., 2003. SlopeAge. University of Cincinnati.

Newton, M.L., Regalla, C.A., Anastasio, D.J., Pazzaglia, F.J., 2005. Bedrock and Surficial Geologic Map of the Monument Hill 7.5′ Quadrangle Southwest Montana. Montana Bureau of Mines and Geology Open File Report 517, scale 1:24, 000, 14 pp.

Olig, S.S., Gorton, A.E., Bott, J.D., 1994. Preliminary interpretations of temporal surface-faulting patterns on the southern Lost River fault zone, northeastern Basin and Range Province, USA. US Geological Survey Open File Report, pp. 145–147.

Olig, S.S., Gorton, A.E., Bott, J.D., Knuepfer, P.L.K., Smith, R.P., Forman, S.L., 1995. Temporal clustering of large earthquakes during the latest Pleistocene on the southern Lost River fault zone, Idaho. Geological Society of America Abstracts with Programs 27, 395.

Olig, S.S., Wong, I.G., Thomas, P.G., Dober, M.C., 2002. Grouping and migration of surface faulting and variations in slip rates on faults in the Great Basin Province. Bulletin of the Seismological Society of America 77, 868–876.

Ostenaa, D., Wood, C., 1990. Seismotectonic study for Clark Canyon Dam, Pick-Sloan Missouri Basin Program, Montana. US Bureau of Reclamation Seismotectonic Report 90–4.

Peacock, D.C.P., 2002. Propagation, interaction and linkage in normal fault systems. Earth-Science Reviews 58, 121–142.

Pierce, K.L., Colman, S.M., 1986. Effect of height and orientation (microclimate) on geomorphic degradation rates and processes, late-glacial terrace scarps in central Idaho. Geologic Society of America Bulletin 97, 869–885.

Pierce, K.L., Morgan, L.A., 1992. The track of the Yellowstone hot spot: volcanism, faulting, and uplift. In: Link, P.K., Kuntz, M.A., Platt, L.B. (Eds.), Regional Geology of Eastern Idaho and Western Wyoming. Geological Society of America Memoir, 179. Geological Society of America, Boulder, CO, pp. 1–51.

Pike, R.J., Wilson, S.E., 1971. Elevation-relief ratio, hypsometric integral, and geomorphic area-altitude analysis. Geological Society of America Bulletin 82, 1079–1083.

Qamar, A.I., Stickney, M.C., 1983. Montana earthquakes, 1869–1979 – historical seismicity and earthquake hazard. Montana Bureau of Mines and Geology Memoir 51, 79.

Regalla, C.A., Reyman, D.K.S., Anastasio, D.J., Pazzaglia, F.J., 2006. Bedrock and surficial geologic map of the Red Rock 7.5′ quadrangle, Beaverhead County, Southwestern Montana. Montana Bureau of Mines and Geology Open File Report 533, scale 1:24, 000, 22 pp.

Schlische, R.W., Young, S.S., Ackermann, R.V., Gupta, A., 1996. Geometry and scaling relations of a population of very small rift-related normal faults. Geology 24, 683–686.

Schmitt, J.G., Haley, J.C., Lageson, D.R., Horton, B.K., Azevedo, P.A., 1995. Sedimentology and tectonics of the Bannanck-McKnight Canyon-Red Butte area, Southwest Montana: new perspectives on the Beaverhead Group and Sevier Orogenic Belt. Northwest Geology 24, 245–313.

Scholten, R.S., Keenmon, K.A., Kupsch, W.O., 1955. Geology of the Lima region, Southwestern Montana and adjacent Idaho. Geological Society of America Bulletin 66, 345–403.

Sears, J.W., Hurlow, H.A., Fritz, W.J., Thomas, R.C., 1995. Late Cenozoic disruption of Miocene grabens on the shoulder of the Yellowstone Hotspot track in southwest Montana; field guide from Lima to Alder, Montana. Northwest Geology 24, 201–219.

Sears, J.W., Fritz, W.J., 1998. Cenozoic tilt domains in southwestern Montana; interference among three generations of extensional fault systems. In: Faulds, J.E., Stewart, J.H. (Eds.), Accommodation Zones and Transfer Zones: the Segmentation of the Basin and Range Province. Geological Society of America Special Paper, 323. Geological Society of America, Boulder, CO, pp. 241–247.

Skipp, B., Perry Jr., W.J., Bartholomew, M.J., Sears, J.W., Johnson, L.M., Dresser, H.H., Hendrix, T.E., O'Neill, M.J., Genovese, P.W., Lageson, D.R., Hanshaw, P.M., 1989. The frontal thrust belt in Montana. In: Schmidt, C.J. (Ed.), Metamorphism and Tectonics of Eastern and Central North America, 1, pp. 83–112.

Snyder, N.P., Whipple, K.X., Tucker, G.E., Merritts, D.J., 2000. Landscape response to tectonic forcing; digital elevation model analysis of stream profiles in the Mendocino triple junction region, Northern California. Geological Society of America Bulletin 112, 1250–1263.

Stein, R.S., 1999. The role of stress transfer in earthquake occurrence. Nature 402, 605–609.

Stickney, M.C., 2000. Quaternary faults and seismicity in Western Montana. Montana Bureau of Mines and Geology, Special Publication 114. 1 sheet, 1:750,000.

Stickney, M.C., Lageson, D.R., 2002. Seismotectonics of the 20 August 1999 Red Rock Valley, Montana earthquake. Bulletin of the Seismological Society of America 92, 2449–2464.

Stickney, M.C., Bartholomew, M.J., Wilde, E.M., 1987. Trench logs across the Red Rock, Blacktail, Lima Reservoir, Georgia Gulch, Vendome and Divide faults, Montana. Geological Society of America Abstracts with Programs, Rocky Mountain Section 19, 336–337.

Strahler, A.N., 1952. Hypsometric (area-altitude curve) analysis of erosional topography. Geological Society of America Bulletin 63, 1117–1141.

Swan, F.H., 1988. Temporal clustering of paleoseismic events on the Oued Fodda Fault, Algeria. Geology 16, 1092–1095.

Wallace, R.E., 1977. Profiles and ages of young fault scarps, north-central Nevada. Geological Society of America Bulletin 88, 1267–1281.

Wallace, R.E., 1987. Grouping and migration of surface faulting and variations in slip rates on faults in the Great Basin Province. Bulletin of the Seismological Society of America 77, 868–876.

Wells, D.J., Coppersmith, K.J., 1994. New empirical relationships among magnitude, rupture length, rupture width, rupture area, and surface displacement. Bulletin of the Seismological Society of America 84, 974–1002.

Whipple, K.X., 2004. Bedrock rivers and the geomorphology of active orogens. Annual Reviews of Earth and Planetary Sciences 32, 155–185.

Zoback, M.L., Zoback, M.D., 1989. Tectonic stress field of the continental United States. In: Pakiser, L.C., Mooney, W.D. (Eds.), Geophysical Framework of the Continental United States. Geological Society of America Memoir, 172. Geological Society of America, Boulder, CO, pp. 523–539.